Preparation of a Unique, Multihollow-Core Honeycomb Structure Via the Unidirectional Freezing of a Binary Solvent System

Rika Okaji, Kentaro Taki, Shinsuke Nagamine, Masahiro Ohshima

Department of Chemical Engineering, Kyoto University, Katsura Campus, Nishikyoku, Kyoto 615-8510, Japan
Correspondence to: R. Okaji (E-mail: okaji@cheme.kyoto-u.ac.jp)

ABSTRACT: Unidirectional freezing is a simple and environmentally friendly method for preparing polymeric porous materials from polymer solutions for use in various applications. In this study, a unique, multihollow-core honeycomb structure was prepared from diurethandimethacrylate (DUDM) in a 1,4-dioxane (Dx) and tertiary butanol (TBA) binary solvent system via unidirectional freezing, subsequent photopolymerization and freeze-drying. The multihollow-core honeycomb consists of two different hollow tubular structures: one structure is noncircular with an atypical cross-sectional area, and the other is circular and measures approximately 5–10 μm in diameter. Both structures are aligned parallel to the freezing direction. These hollow structures were formed by using the sequential growth of Dx and TBA crystals as a template. During the unidirectional freezing process, the Dx crystals grew in the solution along the freezing direction and expelled DUDM and TBA from its crystalline phase into the solution. When the freezing temperature was further decreased, small, needle-shaped TBA crystals grew along the freezing direction and were confined by the Dx crystals. © 2013 Wiley Periodicals, Inc. J. Appl. Polym. Sci. 000: 000–000, 2013

INTRODUCTION

Polymeric porous structures have attracted a lot of attention for use in separation filters,[1,2] drug delivery systems,[3] and bio scaffolds.[4,5] Several preparation methods for polymeric porous materials have been developed, for example, polymer foaming,[6,7] direct printing,[8–10] and templating methods.[2,11,12] Unidirectional freezing is a templating method that utilizes a solvent crystal as the template. This method can be used for various systems, such as particle suspensions,[13–15] sol-gels,[16,17] and polymer solutions.[3,18] Camphene,[14,19] water,[3] and 1,4-dioxane (Dx)[18,20] are generally used as "a template-solvent."

An interesting aspect of using the unidirectional freezing process as a preparation scheme for porous materials is that a wide variety of porous structures, such as planar, lamellar, cellular and dendritic structures, can be produced by controlling the crystal growth behavior via the impurities (e.g., water), freezing rates, and types of solute or solvent used in the process.

For instance, Kim et al. reported that a unidirectionally frozen Dx/(poly L-lactic acid) (PLLA) solution with a small amount of water could form a dendritic structure, while a Dx/PLLA solution without water resulted in a cellular honeycomb monolithic structure.[21] Deville et al. demonstrated that an increase in the freezing rate changed the porous structure from cellular to den-

dritic.[22] An alumina aqueous suspension formed a lamellar structure,[23] whereas polyvinyl alcohol (PVA) aqueous solutions formed a dendritic structure.[3,24] It was also reported that a change in the solvent pH dramatically altered the porous structure from a cellular one to a honeycomb structure.[17]

The formation of these structures during the unidirectional freezing process has been explained by the Mullins and Sekerka[25] theory. This theory proposed that the degree of crystal growth instability at the solid–liquid interface between the solvent crystal and the solution increases when the solution is subjected to steep temperature gradients, large freezing point depressions, impurities or a low-diffusivity solute. The formation of a crystalline structure, for example, planar, lamellar, cellular or dendritic, was attributed to the degree of crystal growth instability.

In this study, we focused on the effect of the crystallizations of binary solvents on the structure during the unidirectional freezing process. The unique needle-like crystal structure of tertiary butyl alcohol (TBA) provided an interesting candidate for investigating the templating ability of crystals for producing porous materials during the freezing process. Because of the desired characteristics of crystal growth,[26] such as the freezing point and high sublimation vapor pressure of the crystal,
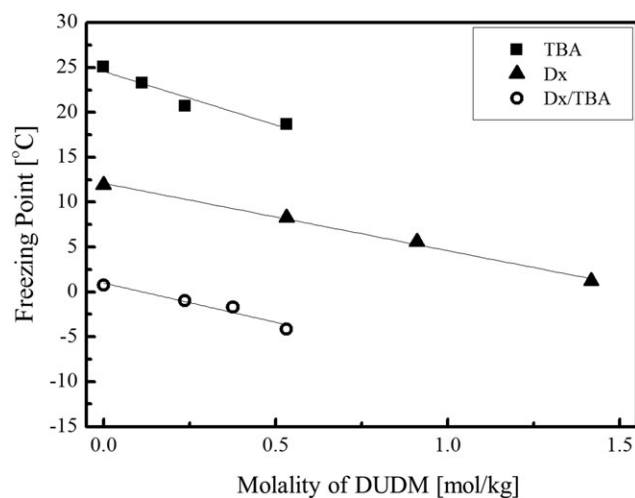
Figure 1. Freezing point-DUDM molality curves for the Dx, TBA, and Dx/TBA mixtures (solid squares: TBA/DUDM solutions, solid triangles: Dx/DUDM solutions, and open circles: Dx/TBA/DUDM solutions).

diurethandimethacrylate (DUDM) was selected as the solute for TBA and Dx. Unidirectional freezing was combined with photopolymerization[27] to determine the crystalline structures that TBA and Dx formed with polymerized DUDM as a template. The porous structures were prepared by unidirectionally freezing and photopolymerizing the TBA/DUDM and Dx/DUDM solutions individually, and both structures were compared with each other in terms of their shapes and sizes. Subsequently, a Dx and TBA binary solvent system was subjected to unidirectional freezing to prepare a multihollow-core honeycomb structure. The difference in the hollow structures between the single solvent systems (TBA/DUDM and Dx/DUDM) was investigated. The freezing point depressions of Dx, TBA and their mixture were also measured to enable the proposal of a unique formation mechanism for the multihollow-core honeycomb structure.

EXPERIMENTAL

Materials
Dehydrated 1,4-Dx and TBA (Wako Pure Chemical Industries) were used as the template solvents. The solute was DUDM (Aldrich), which was used as received. DUDM is highly soluble at room temperature in both Dx and TBA, and mixtures were obtained by gently stirring the materials with a magnetic stirrer for 1 h. Dx/DUDM unary solvent solutions with different DUDM concentrations of 20, 30, and 40 wt % were prepared, and TBA/DUDM unary solvent solutions were also prepared with three different DUDM concentrations: 5, 10, and 20 wt %. For the Dx/TBA binary solvent system, the binary solvent was first prepared with an 80/20 (w/w) ratio, and DUDM was then added to obtain binary solvent solutions with 10, 15, and 20 wt % DUDM. Irgacure 184 (BASF-Japan, Japan) was added as a photoinitiator in a ratio of 1 wt % with respect to DUDM.

Unidirectional Freezing and Photo-Polymerization
The prepared solutions were poured into polypropylene (PP) test tubes at a constant rate of 3.5 cm/h and soaked in a liquid nitrogen bath. The PP test tubes were 1.2-mm thick and 100-

mm long with a 10 mm inner diameter. The tubes were sealed prior to unidirectional freezing. The frozen sample was placed in a cold bath at $-25^{\circ}C$ for 1 h to raise the sample temperature to the photopolymerizable temperature. After removing the test tube from the cold bath, UV light irradiation was immediately conducted for 3 min to solidify the sample. The light source was a mercury xenon lamp (MUV-202U, 200W, MORITEX, Japan). The light intensity at 365 nm was adjusted to 35 mW/cm^2 using a light intensity meter (UT-150, USHIO, Japan). The solidified sample was freeze-dried in a vacuum chamber for 4 days to sublimate the frozen solvents ($-25^{\circ}C$). The porous structure of the obtained samples was observed using field emission scanning electron microscopy (SEM, JEOL-5700, JEOL, Japan). Prior to SEM characterization, the freeze-dried samples were soaked in the liquid nitrogen bath to prevent the samples from deforming during razor blade cutting. The samples were cut either parallel or perpendicular to the freezing direction and were coated using gold-ion sputtering. X-ray computed tomography (FLEX-M543, BEAMSENSE, Japan) was conducted to obtain a three-dimensional (3D) image of the porous structure.

Visual Observations of Dx and TBA Crystal Growth and the Crystal Morphologies
The crystal growth behaviors of Dx and TBA were visually observed. The observations were conducted under a nonunidirectional thermal gradient: the solvents were dropped onto a glass substrate, which was cooled to below -5 °C using a coolant, and the crystallization behavior of the solvents was observed with an optical microscope (KEYENCE, VQ-Z50, Japan). The crystallization behavior of TBA in a confined space was also observed using a microtube (MICROSLIDES, Vitro-Com), which had a rectangular path of 0.05 μm (short axis) by 0.50 μm (long axis). By soaking the microtube in the TBA solution, TBA was introduced into the tube via a capillary force before the tube was placed on the cooled glass substrate. The crystal growth behavior in the tube was observed with the optical microscope.

Table I. Summary of the Cell Morphologies and Freezing Points of the Solutions

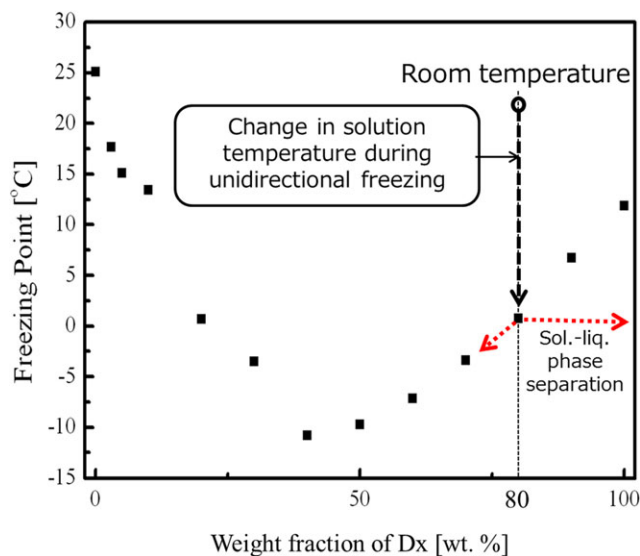| Dx/TBA blending ratio (w/w)	DUDM concentration (wt %)	Cell morphology	Freezing point (°C)
100/0	–	–	11.9
100/0	20	Dendritic	8.28
100/0	30	Dendritic	5.57
100/0	40	Cellular	1.21
80/20	–	–	0.75
80/20	10	Cellular	−1.00
80/20	15	Cellular	−1.69
80/20	20	Cellular	−4.14
0/100	–	–	25.1
0/100	5	Needle	23.25
0/100	10	Needle	20.73
0/100	20	Random	18.67

Figure 2. Freezing points of the Dx/TBA mixtures for different Dx weight fractions. [Color figure can be viewed in the online issue, which is available at wileyonlinelibrary.com.]

Freezing Point Measurements

To investigate the freezing points of the solutions, the solution temperatures were measured in an incubator.[21] The incubator was programmed to decrease its inner temperature from 20°C at a rate of 0.7 K/min. The freezing point was determined to be at the point of the temperature jump, which was caused by the latent heat release.

RESULTS AND DISCUSSION

Freezing Points of the Solutions

The freezing point of each solution was measured and is plotted in Figure 1. The numerical values are listed in Table I along with the cell morphology of the samples prepared by unidirectional freezing. As can be observed in Figure 1, adding DUDM to the Dx and TBA solutions reduced their freezing points. Despite the large DUDM molarity, all of the solutions exhibited a colligative property, that is, the freezing point depression was a linear function of the solute molarity for both the Dx and TBA solutions. The freezing point of the Dx/TBA binary solvent system was between those of Dx and TBA and decreased proportional to the DUDM molarity. The cryoscopic constants,
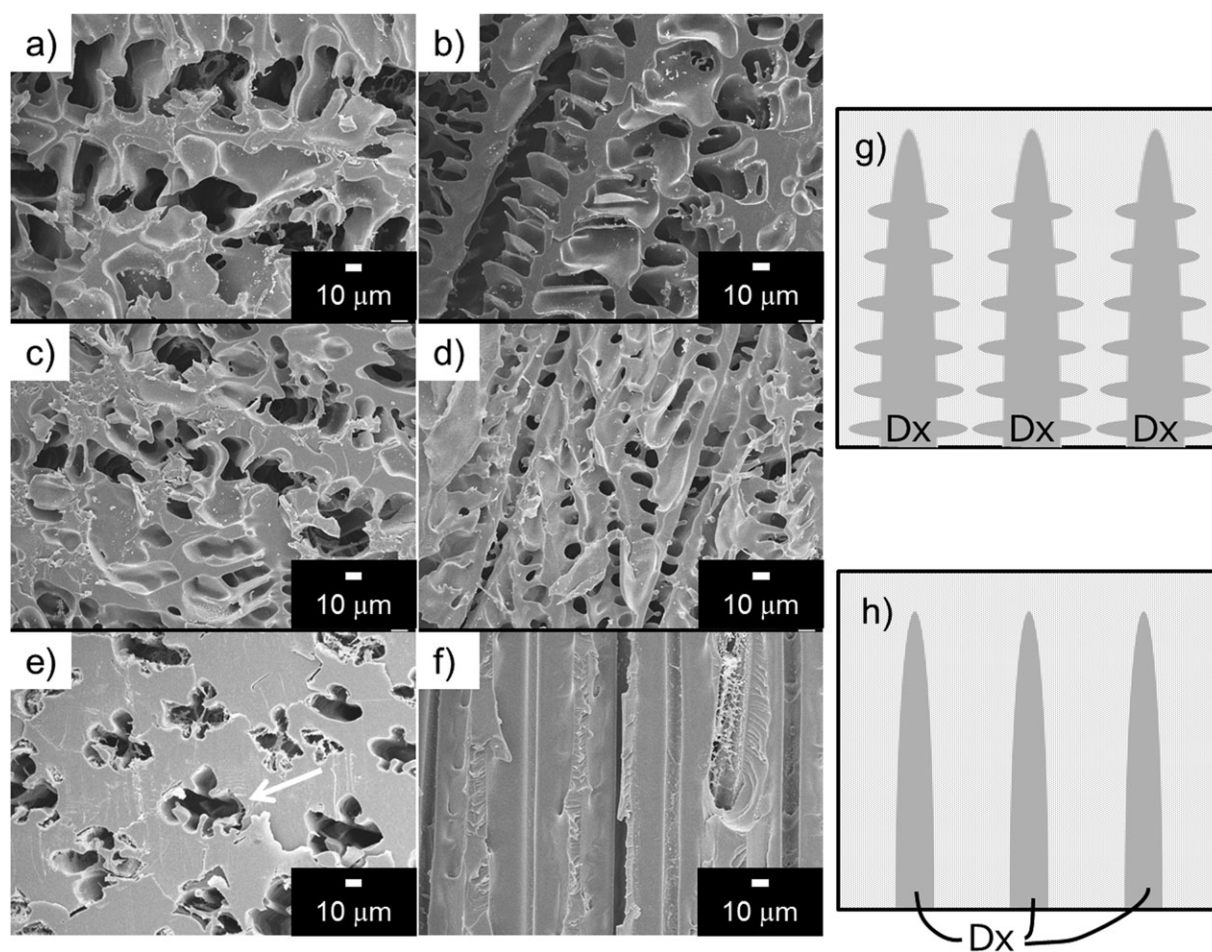

Figure 3. SEM micrographs of the samples prepared from the Dx/DUDM solutions. The cross-sectional views (a, c, and e) were taken perpendicular to the freezing direction, and (b, d, and f) were taken parallel to the freezing direction. The DUDM concentrations were (a and b) 20, (c and d) 30, and (e and f) 40 wt %. (g and h) are the schematic drawing of the Dx crystal growth during unidirectional freezing of Dx/DUDM solution: (g) is the case of 20 or 30 wt % of DUDM concentration, and (h) is 40 wt % of DUDM concentration.

that is, the slopes of the freezing point-solute molarity curves, were 7.32 K·kg/mol for Dx, 18.14 K·kg/mol for TBA and 8.19 K·kg/mol for the Dx/TBA binary solvent. The constant for the Dx/TBA binary solvent system was closer to that of Dx than to that of TBA because the weight fraction of Dx was 0.8.

Figure 2 shows the freezing points of the Dx/TBA mixture for different Dx weight fractions. These mixtures did not contain any DUDM. The freezing points exhibit a V-shaped curve as a function of the Dx weight fraction. The minimum freezing temperature of −10°C was obtained at 40 wt % Dx. These results will be used in a following section to explain the formation mechanism of the multihollow-core honeycomb structure during the unidirectional freezing process.

Porous Structure of the Dx/DUDM Unary Solvent System

Figure 3 shows the SEM micrographs of the porous samples prepared from the Dx/DUDM unary solvent system. The cross-section micrographs (a, c, and e) were taken perpendicular to the freezing direction, while (b, d, and f) were taken parallel to the freezing direction. The DUDM concentrations were 20 wt % for samples (a and b), 30 wt % for (c and d), and 40 wt % for (e and f). A dendritic structure was observed for the 20 and 30 wt % samples and a cellular structure, that is, a smooth wall hollow tube, was observed for the 40 wt % solution samples. The schematics of the crystalline growth behaviors during unidirectional freezing are shown in Figure 3(g,h). In the 20 and 30 wt % DUDM solutions, the trunks of the Dx crystals grew along the freezing direction (bottom to top) and branched perpendicular to the freezing direction. In the 40 wt % DUDM solution, the crystals grew along the freezing direction without branching, as illustrated in Figure 3(h). Generally, a cellular structure can be prepared from dilute and low-viscosity solutions or from low impurity solutions, for example, a low-concentration polymer solution or a colloidal suspension, because the crystal growth instability is reduced by the higher diffusivity and lower degree of freezing point depression of the low solute concentration solutions. However, our experiments showed the opposite result; the cell morphology became cellular with an increase in the solute concentration. Kurz and Fisher[28] discussed the relation between the crystal growth instability and the local freezing point depression at the solidification front. The authors mentioned that when the solute diffusivity is low, a higher solute concentration gradient was established in front of the crystal and increased the degree of crystal growth instability. This theory can be applied to our experimental results. The upper picture in Figure 4 shows typical concentration profiles for the Dx/polymer (solid line) and Dx/DUDM solutions (broken-dotted line) during the unidirectional freezing process; these profiles correspond to the moving solid–liquid interface. Both concentration profiles exhibit the highest concentration at the crystal–solution interface, and the concentrations decrease with increasing distance from the interface due to the solute diffusion in the solution. Assuming that the degree of freezing point depression is proportional to the solute concentration at the interface, the profiles of the freezing point temperature, that is, the profiles of the local solid–liquid equilibrium temperature, are determined, as illustrated in the lower picture of Figure 4. The equilibrium temperature decreased as the solute concentra-
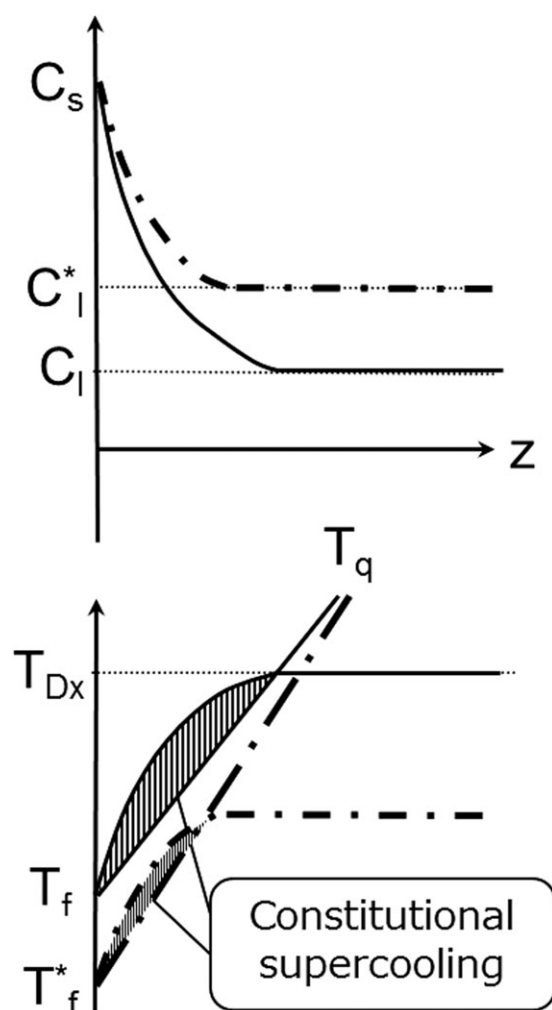

Figure 4. Schematics of the concentration and cryoscopy profiles. Solid line: a typical solvent/polymer solution system. Broken-dotted line: the Dx/DUDM solution. Cs: equilibrium concentration of the solid. Cl: equilibrium concentration of the liquid.

tion increased, following the equation of the colligative property [eq. (1)].

$$T_f = T_f(C_l) - KC_l, \tag{1}$$

where K is the cryoscopic constant of the solvent, and C_l is the weight molar concentration of the solution. T_f is the freezing point temperature.

The curve is a mirror image of the solute concentration profile. The shaded area indicates "constitutional supercooling," in which the solution becomes supercooled, and solvent crystallization is induced. A higher degree of supercooling induces a higher degree of crystal growth instability and changes the crystal growth behavior. Because the solubility of DUDM in the Dx solution is higher than that of most polymers, the bulk concentration of DUDM, C_l, is higher than that of the Dx/polymer system, especially for the 40 wt % DUDM solution, C^*_l. Thus, the freezing point temperature levels out at a lower temperature
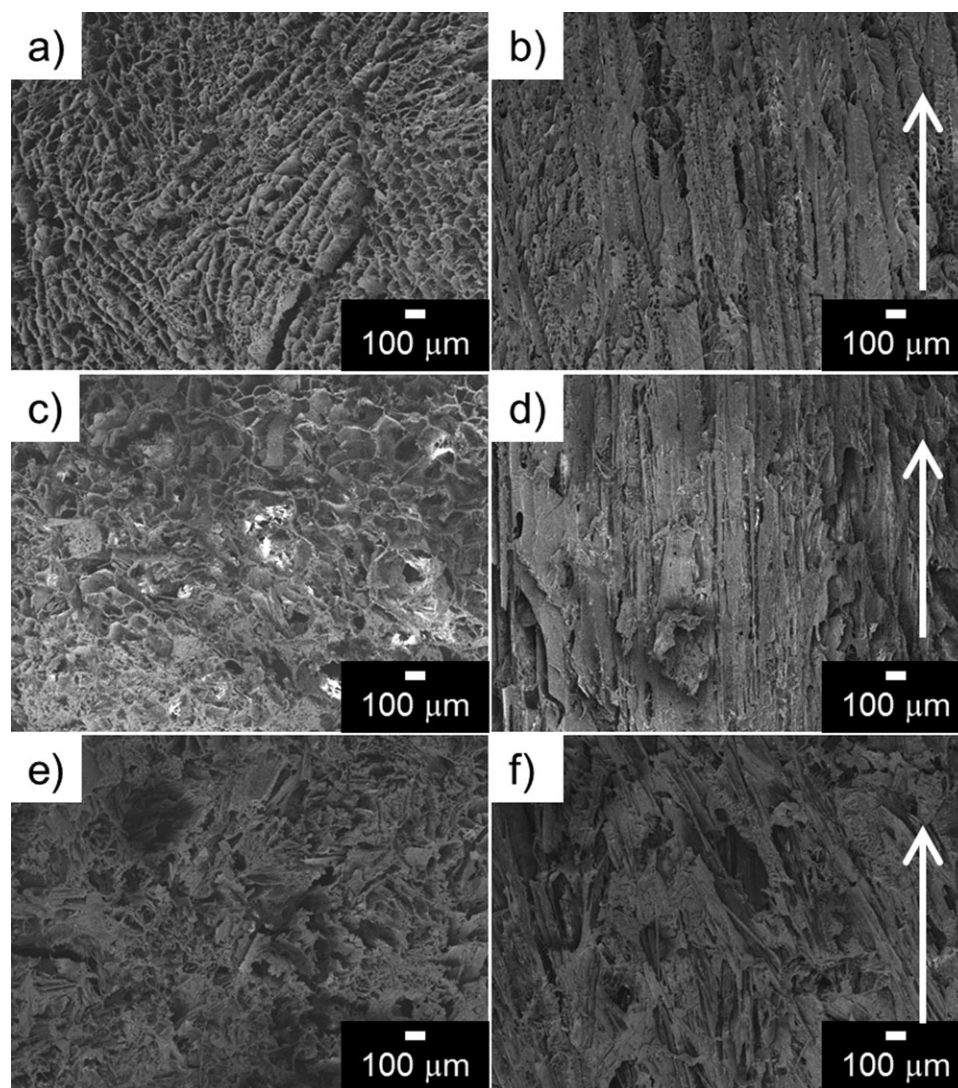
Figure 5. SEM micrographs of the samples prepared from the TBA/DUDM solutions. The cross-sections of the samples were taken (a, c, and e) perpendicular to the freezing direction and (b, d, and f) parallel to the freezing direction. The DUDM concentrations were (a and b) 5, (c and d) 10 and (e and f) 20 wt %. The arrows indicate the freezing direction.

than that of the Dx/polymer system, and the area of constitutional supercooling for the DUDM 40 wt % solution is much smaller than that of the Dx/polymer solution or than that of the other DUDM percentage solutions. When the concentration of the solute ($C^\star_l$) increases, the partition coefficient, that is, the concentration ratio of the solid to the liquid ($C_s/C^\star_l$), the concentration gradient at the freezing front, and the gradient of the freezing point temperature decrease. As a result, the degree of supercooling is decreased when the temperature gradient of the solution is increased due to the depression of the freezing point at the solid–liquid interface. Thus, for the Dx/DUDM solutions, the area of constitutional supercooling narrows when the DUDM concentration is increased to 40 wt %. This phenomenon stabilizes the crystal and produces a cellular crystal for the samples prepared from the Dx/DUDM 40 wt % solution.

Porous Structure of the TBA/DUDM Unary Solvent System

Figure 5 shows the SEM micrographs of the cell morphologies of the samples prepared from the TBA/DUDM unary solvent solutions. The cross-sections (a, c, and e) were taken perpendicular to the freezing direction, and (b, d, and f) were taken parallel to the freezing direction. The DUDM concentrations were 5 wt % for (a and b), 10 wt % for (c and d), and 20 wt % for (e and f). The arrows in the figures indicate the direction of unidirectional freezing.

The observed cell morphologies indicate that the pores were formed with the needle-like crystals of TBA acting as a template. For TBA/DUDM with 5 and 10 wt % DUDM, the pores were formed with a portion being oriented along the unidirectional freezing direction. For the sample prepared from TBA/DUDM with 20 wt % DUDM, the pore orientation became
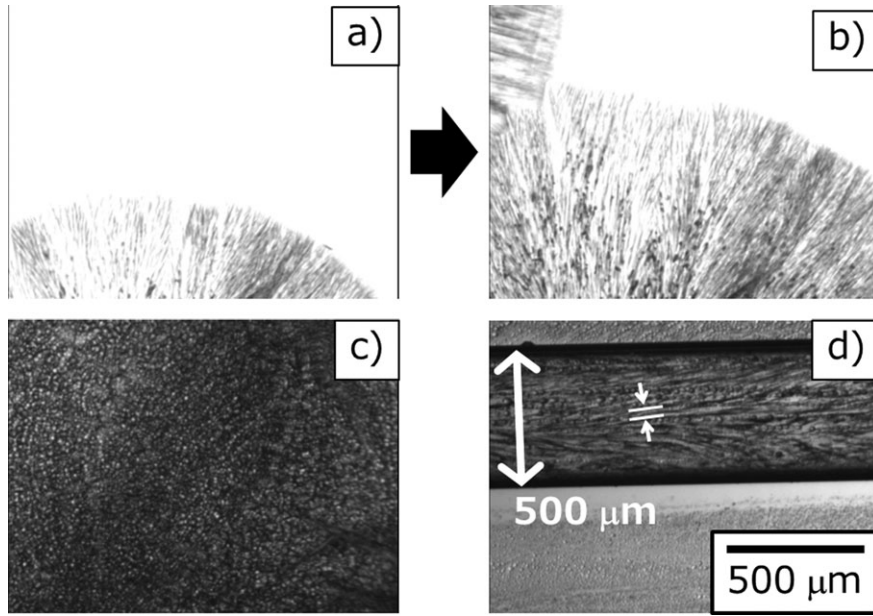
Figure 6. Visual observations of the crystal morphologies of (a, b, and d) TBA and (c) Dx. (a) and (b) show the time lapse of TBA crystallization under a nonunidirectional thermal gradient.
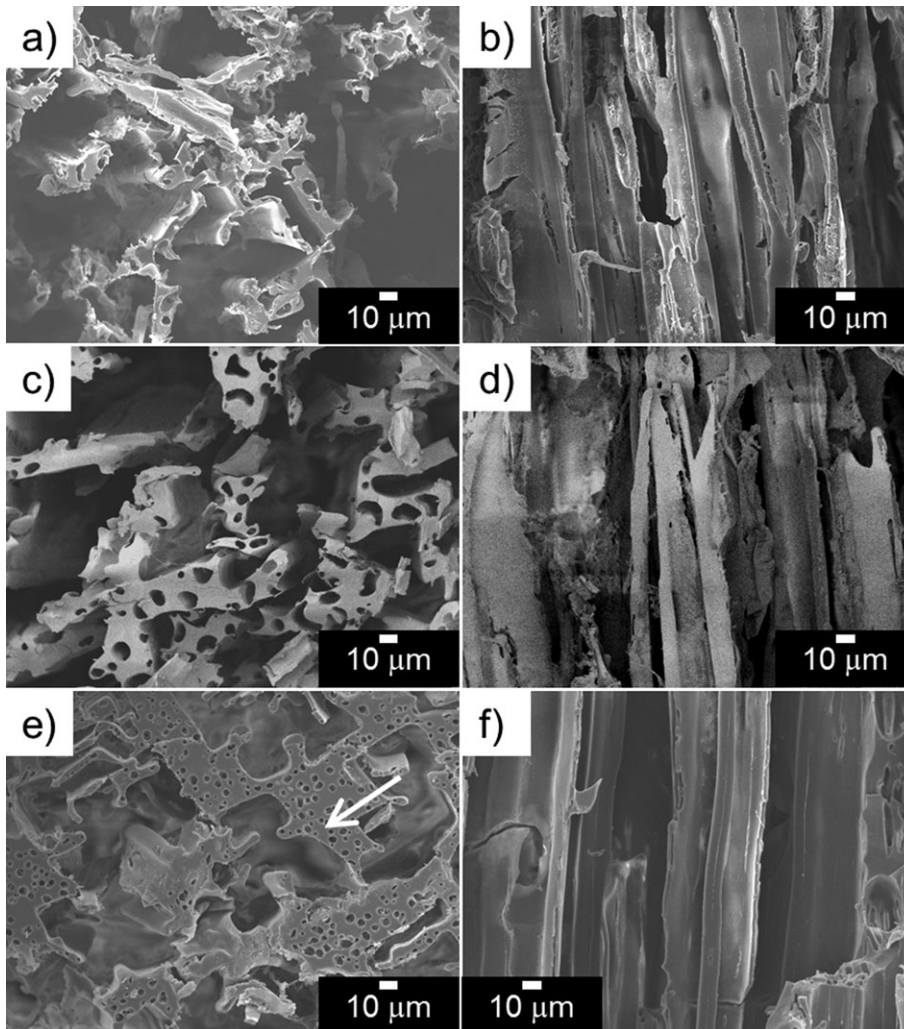

Figure 7. SEM micrographs of the samples prepared from the Dx/TBA/DUDM solutions. The cross-sections samples (a, c, and e) were taken perpendicular to the freezing direction, and (b, d, and f) were taken parallel to the freezing direction. The binary solvent Dx/TBA was mixed in the ratio 80/20 (w/w), and the DUDM concentrations were (a and b) 10, (c and d) 15, and (e and f) 20 wt %.
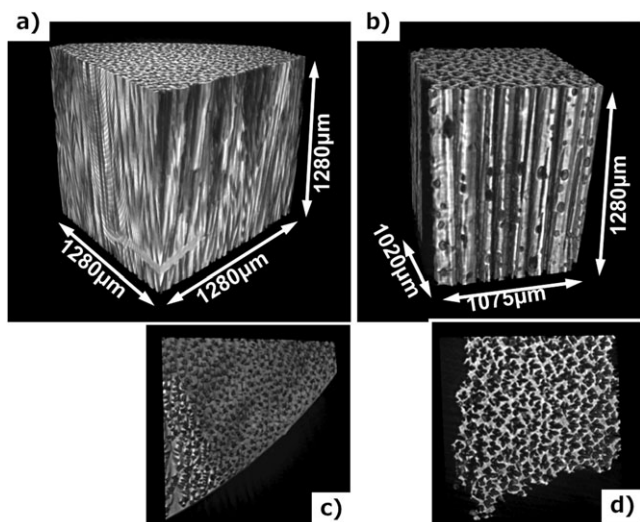
Figure 8. 3D X-ray computed tomography images. (a and c) The Dx single solvent with 40 wt % DUDM. (b and d) The Dx/TBA 80/20 (w/w) binary solvent solution with 20 wt % DUDM. The arrows in (a and b) indicate the direction of unidirectional freezing. (c and d) show the cross-sections taken perpendicular to the freezing direction.

weak, even though each pore shape was still needle-like. It has been reported that the shape of the TBA crystals is needle-like and that the growth rate of the crystals along their long axis is faster than those along their other axes.[26] Therefore, it is highly possible that the TBA crystals grew faster along their long axis than along the unidirectional freezing direction and that this phenomenon and the high viscosity of the 20 wt % solution prevented the crystal growth from being oriented along the freezing direction.

To confirm the TBA crystal shape, visual observations of the crystal growth behavior were conducted. Figure 6(a,b) shows the snapshots of the TBA crystallization behavior on the cooled glass plate. These images show that TBA formed equiaxed needle-like crystals. To compare the crystal shapes, the crystal growth behavior of Dx on the cooled plate was also observed, and one of the snapshots is shown in Figure 6(c). As can be observed, the Dx crystal shape was totally different from that of TBA. Figure 6(d) shows the crystalline morphology of TBA frozen in the microtube. The crystals were aligned along the path of the microtube, and the average diameter of the TBA needle-like crystals in the tube was approximately 8.38 μm.

The results of the visual observations of the TBA crystallization behavior on the cooled glass plate indicate that the needle-like crystals of TBA were not oriented in a specific direction; however, the crystals could be oriented by being grown in tubular spaces.

Porous Structure of the Dx/TBA/DUDM Binary Solvent System

Figure 7 shows the SEM micrographs of the porous structures of the samples prepared from the Dx/TBA/DUDM binary solvent system. The cross-sections (a, c, and e) were taken perpendicular to the freezing direction, and (b, d, and f) were taken

parallel to the freezing direction. The DUDM concentrations of (a and b), (c and d) and (e and f) were 10, 15, and 20 wt %, respectively. The weight ratios of Dx/TBA/DUDM were 72/18/10 (10 wt %), 68/17/15 (15 wt %), and 64/16/20 (20 wt %).

A multihollow-core honeycomb structure was observed for all of the samples. This structure consists of two different hollow tubular structures. One tubular structure is noncircular with an atypical cross-sectional area and is aligned along the freezing direction. As can be observed in Figure 7(a,c,e), the cross-sectional size of the large hollow structure decreased with increasing DUDM concentration. Figure 8 shows the 3D X-ray computed tomography images of the samples prepared from (a) the Dx/DUDM solution with 40 wt % DUDM and (b) the Dx/TBA/DUDM binary solvent solution with 20 wt % DUDM. The X-ray CT images show that both samples have a honeycomb monolithic structure that is oriented along the freezing direction. These morphologies are notably similar to each other. However, Figure 7 clearly shows that the samples prepared from Dx/TBA/DUDM have another hollow structure, which could not be detected by X-ray CT due to the size of the structure. This small hollow structure was circular with a cross-section approximately 5–10 μm in diameter and was aligned along the freezing direction. The walls of the large hollow structure were smooth, which is a feature similar to that of the structure prepared from the Dx/DUDM unary solvent system with 40 wt % DUDM [Figure 3(f)]. A high concentration of DUDM could stabilize the crystal growth, even during the unidirectional freezing process of the Dx/TBA/DUDM binary solvent system. It is reasonable to assume that the large-sized hollow structure is associated with the Dx crystals and that the smaller one is associated with the needle-like TBA crystals.

Formation Mechanism of the Multihollow-Core Honeycomb Structure

The formation mechanism of the multihollow-core honeycomb structure can be considered in the follow way. Figure 2 shows the relation between the freezing point temperature and the concentration ratio of the Dx/TBA binary solution. During the freezing process, the solution temperature decreased from room temperature toward its freezing point, as illustrated by the dashed line in Figure 2. At the freezing point, solid–liquid phase separation occurred, and the crystallization of Dx began. The Dx crystals grew along the freezing direction. The Dx in the solution was consumed for crystal growth, as illustrated in
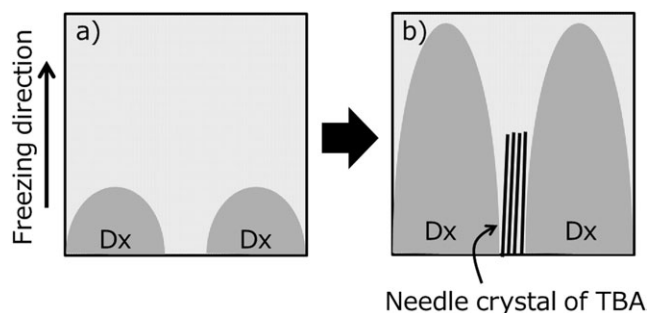

Figure 9. Schematic drawing of the unidirectional crystal growth of the Dx/TBA binary solvent system.
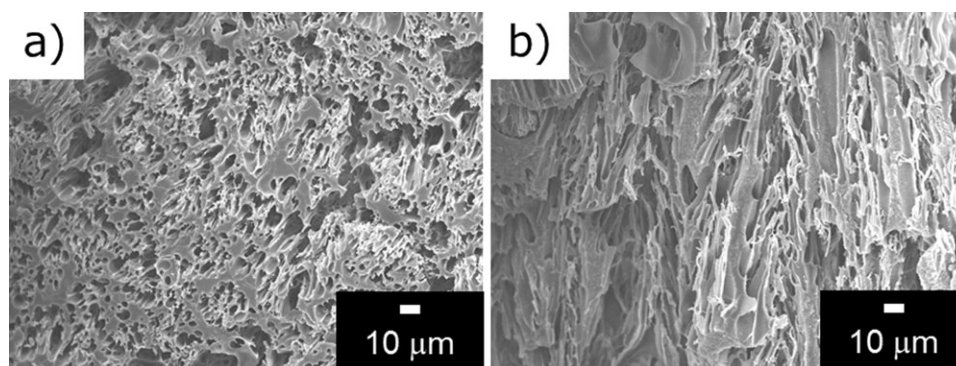
Figure 10. SEM micrographs of the samples prepared from the Dx/TBA/DUDM solutions. The cross-sections were taken (a) perpendicular and (b) parallel to the freezing direction. The binary solvent Dx/TBA was blended in the ratio 50/50 (w/w), and the DUDM concentration was 20 wt %.

Figure 9(a). TBA and DUDM are expelled from the Dx crystal phase. After further lowering the temperature to freeze in the Dx crystallization, the solution became TBA-rich. The crystallization of TBA began when the TBA/DUDM condensed solution temperature was lowered to $-10°C$. As shown in Figure 6(a,b), TBA has a needle-like crystal, which tends to grow equiaxially [Figure 6(b)]; however, in a confined space, such as a microtube, the crystals grow along the guided direction [Figure 6(d)]. During the unidirectional freezing process of the Dx/TBA/DUDM binary solvent system, Dx crystallized first and established crystalline columns, which could confine and guide the growth of the TBA needle-like crystals along the freezing direction, even in the high DUDM concentration solution. This formation mechanism of the multihollow-core structure via the sequential growth of Dx and TBA is illustrated in Figure 9.

To confirm the relation between the cell morphology and the sequence of Dx and TBA crystallization, a Dx/TBA/DUDM solution with a TBA/Dx weight fraction of 50/50 was also unidirectionally frozen to obtain porous samples (Figure 10). Because the 50/50 weight fraction is close to the eutectic point of Dx/TBA, as shown in Figure 2, Dx and TBA started to crystallize at the same time. That is, the needle-like crystals of TBA were formed at the same time that Dx started to crystallize. Therefore, the growth of the TBA crystals was not confined by the Dx crystal columns. The honeycomb structure associated with the Dx crystals, as well as the small hollow structures 5–10 μm in diameter, could not be prepared from the Dx/TBA/DUDM system with a 50/50 TBA/Dx weight fraction.

CONCLUSIONS

Unidirectional freezing of the DUDM solution of the unary solvent systems Dx and TBA and of the binary solvent system Dx/TBA was individually conducted with subsequent photopolymerization. Anisotropic honeycomb structures were obtained. A higher degree of constitutional supercooling directly led to crystal growth instability during the unidirectional freezing process. For conventional polymer/solvent systems, a small amount of impurity or a large amount of solute induce the depression of the freezing point and crystal growth instability. A dendritic structure is formed with an increase in the amount of impurity or solute. A lower-molecular-weight solute, such as DUDM,

exhibits a higher solubility in solvents. This higher solubility reduces the gradient of the freezing temperature profile of the solution at the crystal surface and lowers the degree of constitutional supercooling and the instability of the crystal growth. As a result, a cellular structure can be formed with an increase in the amount of solute. By using two different solvents, a multi-hollow-core honeycomb structure was obtained. This hollow structure was formed by exploiting the sequential growth of Dx and TBA crystals during the unidirectional freezing process and the difference in the crystalline shapes of the two solvents. The experimental results verified that the unidirectionally frozen crystal structure could be controlled by the individual crystal structures of the solvent molecules and by the ratio of the concentrations of the two solvents.

REFERENCES

1. Wood, C. D.; Tan, B.; Trewin, A.; Su, F.; Rosseinsky, M. J.; Bradshaw, D.; Sun, Y.; Zhou, L.; Cooper, A. I. *Adv. Mater.* **2008**, *20*, 1916.

2. Shih, H. C.; Yeh, Y. S.; Yasuda, H. *J. Membrane. Sci.* **1990**, *50*, 299.

3. Gutiérrez, M. C.; García-Carvajal, Z. Y.; Jobbágy, M.; Rubio, F.; Yuste, L.; Rojo, F.; Ferrer, M. L.; del Monte, F. *Adv. Funct. Mater.* **2007**, *17*, 3505.

4. Hua, F. J.; Park, T. G.; Lee, D. S. *Polymer* **2003**, *44*, 1911.

5. Schoof, H.; Apel, J.; Heschel, I.; Rau, G. *J. Biomed. Mater. Res.* **2001**, *58*, 352.

6. Taki, K.; Nitta, K.; Kihara, S.-I.; Ohshima, M. *J. Appl. Polym. Sci.* **2005**, *97*, 1899.

7. Campbell, G. A. *J. Appl. Polym. Sci.* **1972**, *16*, 1387.

8. Kalita, S. J.; Bose, S.; Hosick, H. L.; Bandyopadhyay, A. *Mater. Sci. Eng. C* **2003**, *23*, 611.

9. Teo, E. Y.; Ong, S.-Y.; Khoon Chong, M. S.; Zhang, Z.; Lu, J.; Moochhala, S.; Ho, B.; Teoh, S.-H. *Biomaterials* **2011**, *32*, 279.

10. Zein, I.; Hutmacher, D. W.; Tan, K. C.; Teoh, S. H. *Biomaterials* **2002**, *23*, 1169.

11. Cai, Q.; Yang, J.; Bei, J.; Wang, S. *Biomaterials* **2002**, *23*, 4483.

12. Velev, O. D.; Jede, T. A.; Lobo, R. F.; Lenhoff, A. M. *Nature* **1997**, *389*, 447.

13. Fukasawa, T.; Deng, Z. Y.; Ando, M.; Ohji, T.; Kanzaki, S. *J. Am. Ceram. Soc.* **2002**, *85*, 2151.

14. Araki, K.; Halloran, J. W. *J. Am. Ceram. Soc.* **2004**, *87*, 1859.

15. Chino, Y.; Dunand, D. C. *Acta Mater.* **2008**, *56*, 105.

16. Deville, S.; Saiz, E.; Tomsia, A. P. *Biomaterials* **2006**, *27*, 5480.

17. Mukai, S. R.; Nishihara, H.; Tamon, H. *Micropor. Mesopor. Mater.* **2003**, *63*, 43.

18. Kim, J. W.; Taki, K.; Nagamine, S.; Ohshima, M. *Langmuir* **2009**, *25*, 5304.

19. Koh, Y. H.; Lee, E. J.; Yoon, B. H.; Song, J. H.; Kim, H. E.; Kim, H. W. *J. Am. Ceram. Soc.* **2006**, *89*, 3646.

20. Ma, P. X.; Zhang, R. Y. *J. Biomed. Mater. Res.* **2001**, *56*, 469.

21. Kim, J. W.; Taki, K.; Nagamine, S.; Ohshima, M. *Chem. Eng. Sci.* **2008**, *63*, 3858.

22. Deville, S.; Saiz, E.; Tomsia, A. P. *Acta Mater.* **2007**, *55*, 1965.

23. Deville, S. *Adv. Eng. Mater.* **2008**, *10*, 155.

24. Zhang, H. F.; Hussain, I.; Brust, M.; Butler, M. F.; Rannard, S. P.; Cooper, A. I. *Nat. Mater.* **2005**, *4*, 787.

25. Mullins, W. W. Sekerka, R. F. *J. Appl. Phys.* **1964**, *35*, 8.

26. Fabietti, L. M.; Trivedi, R. *J. Cryst. Growth* **1997**, *182*, 185.

27. Okaji, R.; Taki, K.; Nagamine, S.; Ohshima, M. *J. Appl. Polym. Sci.* **2012**, *125*, 2874.

28. Kurz, W.; Fisher, D. J. Fundamentals of Solidification, 4th ed.; Trans Tech Publication Ltd: Switzerland, **1998**.